Multi-biomarker pharmacokinetic-pharmacodynamic relationships of central nervous systems active dopaminergic drugs

Brink, W.J. van den

CHAPTER 7

BLOOD-BASED BIOMARKERS OF QUINPIROLE PHARMACOLOGY: MULTIVARIATE PK/PD AND METABOLOMICS TO UNRAVEL THE UNDERLYING DYNAMICS IN PLASMA AND BRAIN

W.J. van den Brink, R. Hartman, D.J. van den Berg, G. Flik, B. Amoros-Gonzalez, N. Koopman, J. Elassais-Schaap, P.H. van der Graaf, T. Hankemeier, E.C.M. de Lange

Submitted to CPT:PSP

Abstract

A key challenge in the development of CNS drugs is the availability of drug target specific blood-based biomarkers. As a new approach, we applied multivariate pharmacokinetic/pharmacodynamic (PK/PD) analysis in $brain_{ECF}$ and plasma simultaneously after 0, 0.17 and 0.86 mg/kg of the dopamine $D_{2/3}$ agonist quinpirole (QP) in rats. We measured 76 biogenic amines in plasma and $brain_{ECF}$ after single and 8-day administration, to be analyzed by multivariate PK/PD analysis. Multiple concentration-effect relations were observed with potencies ranging from 0.001 – 383 nM. Many biomarker responses propagated over the blood-brain-barrier. Effects were observed for dopamine and glutamate signaling in $brain_{ECF}$, and branched-chain amino acid metabolism and immune signaling in plasma. Altogether, we showed for the first time how multivariate PK/PD could describe a systems-response across plasma and brain, thereby identifying potential blood-based biomarkers. This concept is envisioned to provide an important connection between drug discovery and early drug development.

Keywords: Metabolomics, systems pharmacology, PK/PD, CNS drug development, dopamine agonists

Introduction

One of the key challenges in central nervous system (CNS) drug development is the discovery of blood-based biomarkers that reflect the central response (1,2). Such biomarkers enhance the evaluation of the proof of pharmacology of CNS drugs, which is crucial for successful drug development (3). It is particularly important to dynamically evaluate the biomarker responses in relation to the systems pharmacokinetics (PK) of the drug, given that the interaction between PK and pharmacodynamics (PD) typically is non-linear and time-dependent (4,5).

While currently biomarker discovery is nowadays typically driven by the known pharmacological mechanisms, metabolomics fingerprinting is not limited to these pathways. Metabolomics analysis has revealed multiple new biochemical pathways in relation to drug responses (6–11).

One of the techniques being useful in CNS biomarker discovery is intracerebral microdialysis. It is a well-established technique that has been successfully applied to study drug concentrations as well as drug response biomarkers in brain extracellular fluid ($brain_{ECF}$) to evaluate CNS PK and PD (12–14). Therefore, microdialysis is the method of choice to dynamically evaluate a metabolomics fingerprint in brain extracellular fluid ($brain_{ECF}$) simultaneously upon CNS drug treatment. Such dynamical evaluation would improve the quantitative insights into systems-wide responses (i.e. changes in biomarker concentrations), thereby shifting CNS drug development from an empirical towards a mechanistic discipline (15,16).

In an earlier study we have already shown that a multivariate (PK/PD) evaluation of a metabolomics response in plasma reveals multiple dynamics underlying a systems response upon treatment with remoxipride (17). In the current study we set out to extend this methodology with a simultaneous evaluation of a metabolomics response in both plasma and $brain_{ECF}$, using the dopamine $D_{2/3}$ receptor agonist quinpirole (QP) as paradigm compound. Overall, the purpose is to provide insight into the systems-wide biochemical responses of CNS drugs, combined with PKPD modeling as a new approach to discover blood-based biomarkers of central responses.

Methods

Animals, surgery and experiment

Animals – Animal studies were performed in agreement with the Dutch Law of Animal Experimentation and approved by the Animal Ethics Committee in Leiden, the Netherlands (study protocol DEC12247). For details on animals, surgery and experiment, we refer to (18).

Surgery – In short, male Wistar rats (n=44) underwent surgery while anesthetized, to receive cannulas in the femoral artery and vein for blood sampling and drug administration, respectively. The microdialysis probe guides (CMA/12) and their dummy probes were implanted in the caudate putamen in both hemispheres. The probes (CMA/12 – Elite 4 mm) were placed 24 hours before experiment.

Experiment – The animals were subjected to an experiment on two days with 7 days in between. On the days of experiment, the rats were randomly assigned to receive 0 mg/kg (n=12), 0.17 mg/kg (n=16) or 0.86 mg/kg (n=16) QP. Microdialysate samples were collected from -200 to 180 minutes (20-minute interval, 1.5 µl/min, 120 min. equilibration time). Blood samples were taken at -5, 5, 7.5, 10, 15, 25, 45, 90, 120 and 180 minutes and centrifuged to separate the plasma (1000 x g, 10 min, 4°C). Samples were stored at -80°C until analysis. Between the experiment days, the same doses were administered subcutaneously.

Chemical analysis of the samples

Targeted monoamine + metabolite analysis – A selection of plasma and microdialysate samples collected on experiment day 1 were analyzed by BrainsOnline (Groningen, The Netherlands). The samples were delivered on dry ice and stored at -80°C until analysis. Monoamines and their metabolites (serotonin, 5-hydroxy indoleacetic acid, dopamine, 3,4-hydroxyphenylacetic acid, homovanillic acid, glutamate and glycine) were analyzed employing SymDAQ derivitization (19,20). Data were calibrated and quantified using the Analyst™ data system (Applied Biosystems, Bleiswijk, The Netherlands) to report concentrations of the analytes.

Untargeted biogenic amine analysis – The biogenic amines were analyzed in microdialysate and plasma samples of experiment day 1 and 8 according to a previously described method (21). Amino acids and amines were derivatized by an Accq-tag derivatization strategy. Plasma samples (5 µL) were reduced with TCEP (tris(2-carboxyethyl)phosphine) and deproteinated by MeOH. Microdialysate samples (30 µL) were only reduced with TCEP. The samples were dried under vacuum while centrifuged (9400xg, 10 min, Room Temperature), and reconstituted in borate buffer (pH 8.8) with with AQC (6-aminoquinolyl-N-hydroxysuccinimidyl carbamate) derivatization reagent. The reaction mixtures were injected (1 µL) into an UPLC-MS/MS system, consisting of an Agilent 1290 Infinity II LC system, an Accq-Tag Ultra column, and a Sciex Qtrap 6500 mass spectrometer. The peaks were assigned using Sciex MultiQuant software, integrated, normalized for their internal standards, and corrected for background signal. Only compounds with a QC relative standard deviation (RSD_{QC}) under 30% were reported to assure quality of the data.

Data analysis

Pharmacokinetic model – The PK model has been published previously and described the free QP concentrations in plasma and brain$_{ECF}$ with QP doses ranging from 0.17 to 2.14 mg/kg (18).

Pharmacodynamic models – A PD model was developed for each single metabolite (hereafter called biomarkers) using a population approach in NONMEM® version 7.3.0 with subroutine ADVAN13. The inter-individual variability around the parameters and the residual error were described by an exponential distribution (suppl. Equation 1, 2). A combination of submodels was evaluated for each single biomarker consisting of i) a straight baseline, an exponential decay, or a linear slope model; ii) a linear or a sigmoid E_{MAX} concentration response model; iii) a transit or no transit compartment model; and iv) a turnover or a pool model (Suppl. equations 4 - 7). In addition, a model with no drug response function was evaluated (Suppl. equation 8) The models were selected on basis of the objective function value (χ^2-test, $p < 0.05$), the condition number, successful convergence and visual evaluation of goodness-of-fit plots.

Exploration of target site – For biomarkers showing a response in either plasma or brain$_{ECF}$, the site with the response was identified as effect target site. In case a biomarker showed a response both in plasma and brain$_{ECF}$, two PD models were developed with either the plasma biomarker response driving the brain$_{ECF}$ biomarker response or vice versa. The link between the response in plasma and brain$_{ECF}$ was described by a linear or a non-linear brain transport model following Michaelis Menten kinetics (Suppl. Equation 9). The Aikaike Information Criterium (AIC) of the 'brain$_{ECF}$ target site model' was subtracted from that of the 'plasma target site model' to calculate the ΔAIC for selection of the target site model. A negative ΔAIC indicated plasma as target site of effect, while a positive ΔAIC suggested brain$_{ECF}$ as target site of effect.

Clustering – The longitudinal biomarker responses were simulated for their determined target site and subsequently clusters of the dynamical pharmacological responses were identified in plasma and brain$_{ECF}$ using k-means clustering. The number of clusters was selected in two steps. First an elbow plot, depicting number of clusters against within cluster sum of squares, was used to identify a range of potential number of clusters. Second, for each potential number of clusters a PK/PD cluster model was developed describing the cluster responses. The AIC was used to select the model with the optimal number of clusters. Subsequently, a step-wise parameter sharing procedure was applied as previously described (17). In short, a single parameter (e.g. EC_{50}) was estimated for multiple clusters and evaluated by the change in OFV (χ^2-test, $p < 0.05$) to determine whether this was statistically different from a model with separate parameters. If no difference was found, the shared parameter was kept in the model.

Significance score calculation - The cluster-based model was compared to a model with no drug effect model included, i.e. assuming no effect of QP. A significance score was calculated by the change in OFV corrected for the degrees of freedom with a Bonferroni-corrected significance threshold of $\alpha = 0.01$ (Suppl. equation 10). A significance score > 0 reflects a significant effect of QP on a biomarker response.

Effect of eight-day QP administration

Basal biomarker levels (t = 0) in both $brain_{ECF}$ and plasma at experiment day 1 and experiment day 8 were compared using two-way ANOVA with interaction between dose and experiment day. Tukey honest significant different test was used for posthoc analysis. $Brain_{ECF}$ basal biomarker levels were averaged per animal, given that there were 4-6 baseline samples for each animal. For the biomarkers that revealed a significant change with experiment day, a covariate analysis was performed in the single biomarker models by estimating a separate baseline parameter per combination of treatment group and experiment day. Only if the covariate analysis revealed a difference, the effect was considered significant.

Results

Exploration of target site of effect

The metabolomics data revealed 23 biomarkers primarily responding to QP in plasma, and 15 biomarkers primarily affected by QP in the brain (Table I, Figure 1). DL-3-aminobutyric acid and serotonin could only be measured in plasma, while L-glutamine could only be measured in $brain_{ECF}$. From all the biomarkers that reflected an effect of plasma QP, 19 showed a net transport to the $brain_{ECF}$. Inversely, 5 biomarkers exhibited a net transport from $brain_{ECF}$ into plasma, potentially leading to secondary responses in plasma. The inter-compartmental transport rates between plasma and $brain_{ECF}$ of many biomarkers were described by non-linear Michaelis-Menten kinetics (Table I).

Table I. Overview of biogenic amines and their target site that showed a response upon QP treatment. The Delta Akaike Information Criterium (ΔAIC) indicates the target site (see methods). Also, the type of brain transport is indicated (yes, no or not available (N.A.)). PàB and BàP stand for plasma-to-brain and brain-to-plasma, respectively. Only biomarkers presented in black showed a significant response in the cluster models.

Biomarker	Target site	ΔAIC	Brain transport
	Targeted approach (BrainsOnline)		
Dopamine	$Brain_{ECF}$	-	No
DOPAC	$Brain_{ECF}$	-	No
HVA	$Brain_{ECF}$	-	No
Glycine	Plasma	-56.216	Yes – $NonLin_{PàB}$
5-HIAA	Plasma	-	No
L-Glutamic acid	Plasma	-	No

Table I. (continued)

Biomarker	Target site	ΔAIC	Brain transport
	Untargeted approach (BMFL)		
L-Phenylalanine	Plasma	-75.811	Yes – $NonLin_{BaP}$
L-Valine	Plasma	-73.682	Yes – $NonLin_{BaP}$
L-Methionine sulfoxide	Plasma	-55.917	Yes – $NonLin_{PaB}$
Taurine	Plasma	-48.638	Yes – $NonLin_{BaP}$
S-Methylcysteine	Plasma	-46.564	Yes – Linear
L-Alpha-aminobutyric acid	Plasma	-40.634	Yes – $NonLin_{PaB}$
L-Asparagine	Plasma	-37.597	Yes – $NonLin_{BaP}$
L-Alanine	Plasma	-35.086	Yes – $NonLin_{PaB}$
Gamma-L-glutamyl-L-alanine	Plasma	-33.872	Yes – $NonLin_{PaB}$
L-Threonine	Plasma	-31.734	Yes – Linear
L-Methionine	Plasma	-24.946	Yes – Linear
L-Histidine	Plasma	-24.715	Yes – Linear
L-Arginine	Plasma	-24.469	Yes – $NonLin_{PaB}$
L-Isoleucine	Plasma	-13.582	Yes – $NonLin_{BaP}$
Glycine	Plasma	-12.572	Yes – Linear
Homocysteine	Plasma	-10.954	Yes – Linear
L-Serine	Plasma	-8.129	Yes – Linear
Citrulline	Plasma	-5.407	Yes – $NonLin_{BaP}$
L-Leucine	Plasma	-2.462	Yes – $NonLin_{BaP}$
DL-3-aminoisobutyric acid	Plasma	-	N.A.
Histamine	Plasma	-	No
L-Glutamic acid	Plasma	-	No
L-Homoserine	Plasma	-	No
Methionine sulfone	Plasma	-	No
Serotonin	Plasma	-	N.A.
L-Proline	$Brain_{ECF}$	41.574	Yes – $NonLin_{BaP}$
N6,N6,N6-Trimethyl-L-lysine	$Brain_{ECF}$	27.282	Yes – $NonLin_{BaP}$
Hydroxylysine	$Brain_{ECF}$	8.103	Yes – Linear
L-Lysine	$Brain_{ECF}$	4.747	Yes – $NonLin_{BaP}$
L-4-hydroxy-proline	$Brain_{ECF}$	1.111	Yes – $NonLin_{BaP}$
Homocitrulline	$Brain_{ECF}$	0.261	Yes – $NonLin_{BaP}$
3-Methoxytyramine	$Brain_{ECF}$	-	No
5-Hydroxy-L-tryptophan	$Brain_{ECF}$	-	No
Cystathionine	$Brain_{ECF}$	-	No
Gamma-aminobutyric acid	$Brain_{ECF}$	-	No
L-2-aminoadipic acid	$Brain_{ECF}$	-	No
L-Glutamine	$Brain_{ECF}$	-	N.A.
L-Tryptophan	$Brain_{ECF}$	-	No
L-Tyrosine	$Brain_{ECF}$	-	No
Ornithine	$Brain_{ECF}$	-	No
Putrescine	$Brain_{ECF}$	-	No
Sarcosine	$Brain_{ECF}$	-	No

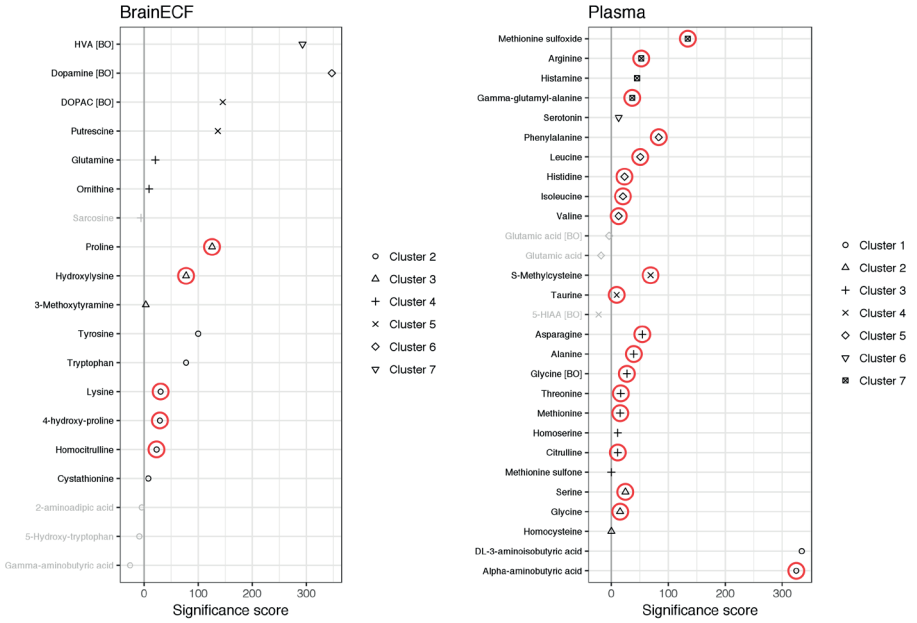

Figure 1. Significance score of responding metabolites in brain$_{ECF}$ (left) and plasma (right) indicating their potential as a biomarker of the QP systems effect. The grey line marks the significance threshold; metabolites right of the line were significantly affected by QP. The red circles indicate the metabolites that distribute from brain$_{ECF}$ to plasma and vice versa. *Cluster 1 was excluded for brain$_{ECF}$ since no effect was observed. [BO] refers to the amines analyzed by BrainsOnline.

Clustered response patterns in brain$_{ECF}$ and plasma

A total of 7 clusters of dynamical biomarker responses in brain$_{ECF}$ was selected (Table II). Using parameter sharing, it was observed that the biomarkers responded with either a high or a low potency (EC_{50} = 0.01 nM or EC_{50} = 122 nM, Table III, Figure 2). The turnover of these biomarkers was low (0.031 min^{-1} – 0.056 min^{-1}) or high (0.13 min^{-1} – 0.44 min^{-1}). The responses in plasma were also separated into 7 clusters (Table II) described by models with transit compartment models (cluster 1 & 4), pool models (cluster 5 & 6) and turnover models (cluster 2, 3 & 7) (Table III). A wider variety of potency parameter estimates were identified in plasma as compared to brain$_{ECF}$: 0.01 nM, 17.2 nM, and 113 - 383 nM (Table III, Figure 2). Moreover, the direction of response was both up (cluster 1 & 4) and down (cluster 2, 3 & 5-7). The responses in brain$_{ECF}$ and plasma were well described by the cluster-PKPD models (Figure 3, suppl. Figure 2).

Effect of QP on the dopamine pathway

Dopamine (DA), 3,4-dihydroxyphenylacetic acid (DOPAC), and homovanillic acid (HVA), the key constituents of the dopamine pathway, were decreased in brain$_{ECF}$ upon QP treatment. Whereas the *in vivo* potency was found to be similar for these biomarkers (122 nM), the

Table II. Determination of optimal number of clusters in plasma and brain$_{ECF}$ using the Akaike Information Criterium (AIC). In bold the selected number of clusters.

Plasma		Brain$_{ECF}$	
# clusters	**AIC**	# clusters	**AIC**
4	65500.76	6	78140.64
5	64991.03	**7**	**76518.12**
6	64966.79	8	76523.49
7	**64876.42**	9	78319.55
8	66314.62	10	76535.81

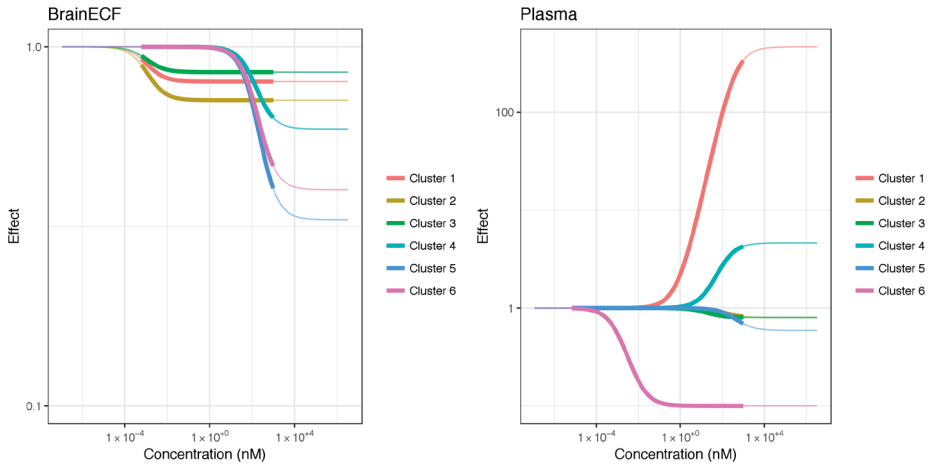

Figure 2. An overview of the concentration-effect relations that underlie the systems responses in brain$_{ECF}$ (left) and plasma (right). Thick line parts represent the range of observed biomarker concentrations *Cluster 1 was excluded for brain$_{ECF}$ since no effect was observed.

maximal inhibition values (DA: 67%, DOPAC: 41%, HVA: 60%) and the turnover rates (DA: 0.44 min^{-1}, DOPAC: 0.13 min^{-1}, HVA: 0.031 min^{-1}) were different (Table III, Figure 2). No responses of QP treatment were observed for DA and HVA in plasma, while DOPAC could not be measured in plasma due to assay lower limit of detection of 50 nM.

Table III. Parameter estimates of the cluster models. RSE: relative standard error.

Plasma		Brain$_{ECF}$	
Parameter	**Estimate (RSE)**	**Parameter**	**Estimate (RSE)**
	*Cluster 1**		
E_{MAX} (%)	4650 (41.1%)		
EC_{50} (nM)	383 (54.3%)		
k_{out} (min^{-1})	0.035 (42.3%)		
$k_{transit}$ (min^{-1})	0.044 (33.1%)		

$n_{transit}$	8.3 (19.2%)		
	Cluster 2		
I_{MAX} (%)	-20 (30.1%)	I_{MAX} (%)	-20 (6.1%)
IC_{50} (nM)	113 (98.5%)	IC_{50} (nM)	0.001 (fix)
k_{out} (min^{-1})	0.057(38.3%)	k_{out} (min^{-1})	0.056 (27.9%)
	Cluster 3		
I_{MAX} (%)	-20 (30.1%)	I_{MAX} (%)	-29 (7.1%)
IC_{50} (nM)	17.2 (50.6%)	IC_{50} (nM)	0.001 (fix)
k_{out} (min^{-1})	0.11 (12.2%)	k_{out} (min^{-1})	0.13 (13.3%)
	Cluster 4		
E_{MAX} (%)	363 (67.5%)	I_{MAX} (%)	-15 (13.5%)
EC_{50} (nM)	113 (98.5%)	IC_{50} (nM)	0.001 (fix))
k_{out} (min^{-1})	9.58 (104%)	k_{out} (min^{-1})	0.14 (32.7%)
$k_{transit}$ (min^{-1})	0.0052 (46.8%)		
$n_{transit}$	1.79 (17.9%)		
	Cluster 5		
I_{MAX} (%)	-41 (14.6%)	I_{MAX} (%)	-41 (9.0%)
IC_{50} (nM)	339 (32.8%)	IC_{50} (nM)	122 (51.4%)
k_{out} (min^{-1})	0.11 (12.5%)	k_{out} (min^{-1})	0.13 (13.3%)
k_{rel} (min^{-1})	0.018 (27.5%)		
	Cluster 6		
I_{MAX} (%)	-90 (0.3%)	I_{MAX} (%)	-67 (4.9%)
IC_{50} (nM)	0.001 (fix)	IC_{50} (nM)	122 (51.4%)
k_{out} (min^{-1})	0.10 (18.4%)	k_{out} (min^{-1})	0.44 (47.9%)
k_{rel} (min^{-1})	0.35 (19.6%)		
	Cluster 7		
I_{MAX} (%)	-41 (6.4%)	I_{MAX} (%)	-60 (9.3%)
IC_{50} (nM)	17.2 (50.6%)	IC_{50} (nM)	122 (51.4%)
k_{out} (min^{-1})	0.060 (13.5%)	k_{out} (min^{-1})	0.031 (28.9%)

*** Cluster 1 was excluded for $brain_{ECF}$ since no dose-response was observed. Consequently, parameter estimates were not informative.**

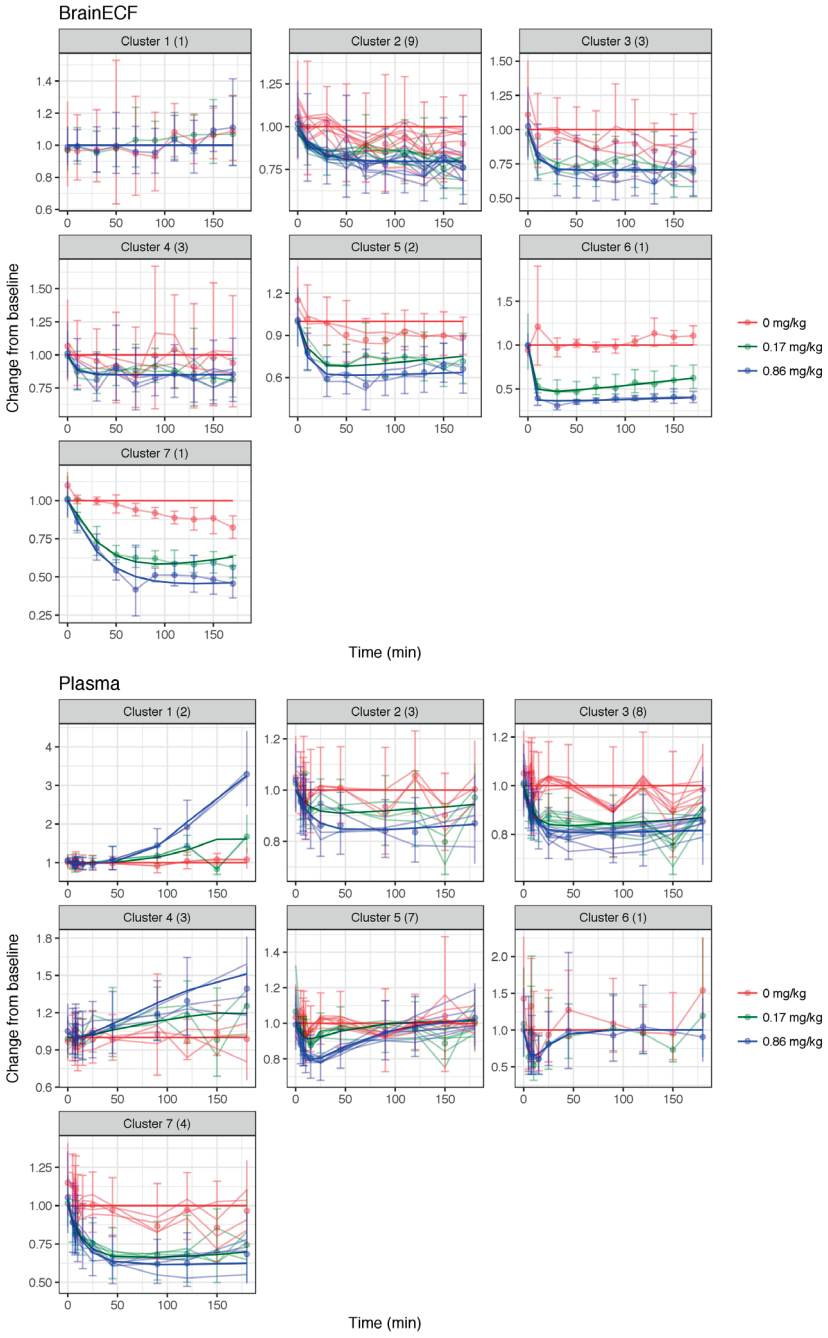

Figure 3. Goodness-of-fit of the cluster responses as change from baseline in brain$_{ECF}$ (top) and plasma (bottom). Dots and error bars mark the geometric mean +/- standard deviation of the observed cluster responses, light lines represent the geometric mean of the single metabolite responses and dark lines show the predicted cluster responses. The facet labels show the number of metabolites between the parentheses.

Effect of QP on other pathways in brain$_{ECF}$

In brain$_{ECF}$ QP was found to interact with the polyamine metabolism (ornithine, putrescine), the proline metabolism (proline, L-4-hydroxyproline), neurotransmitter precursors (tryptophan, tyrosine), and lysine metabolism (lysine, hydroxylysine) (Table I, Figure 1).

Effect of QP on metabolic pathways in plasma

The systemic response on amino acid metabolism in plasma indicated interactions between QP and the branched chain amino acid (BCAA) metabolism (leucine, isoleucine, valine), neurotransmitter synthesis (phenylalanine), serine-glycine-threonine metabolism (serine, glycine, threonine), and histamine metabolism (histidine, histamine) (Table I, Figure 1). Furthermore, alpha-aminobutyric acid and DL-3-aminoisobutyric acid strongly responded to QP treatment (Table I, Figure 1).

Effect of eigth-day QP administration on basal biomarker levels

Eight-day QP administration did not result in significant changes in basal brain$_{ECF}$ biomarker levels, but showed a significant change in plasma levels of alpha-aminobutyric acid and DL-3-aminoisobutyric acid after 0.17 mg/kg ($p < 0.05$), but not after 0.86 mg/kg QP ($p > 0.05$) (Figure 4). However, including the interaction between treatment and day as a covariate in the PK/PD models for these biomarkers did not result in a significant improvement of the model ($p > 0.05$), potentially related to the lack of a dose-response relation.

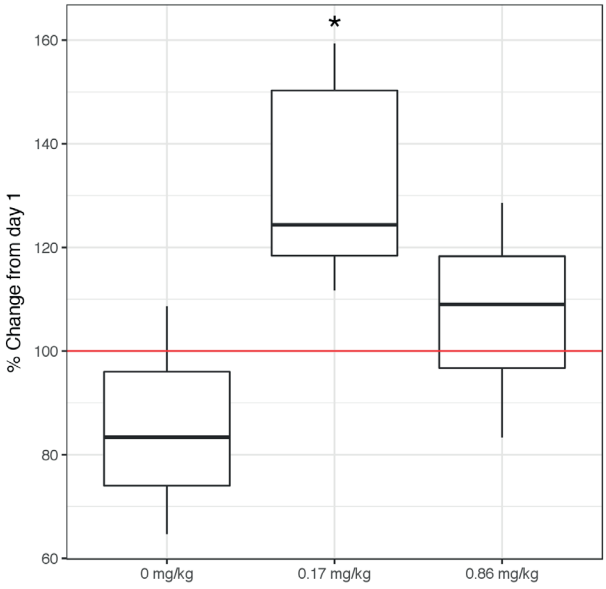

Figure 4. Relative change of L-Alpha-aminobutyric acid levels in plasma after 8-day administration as compared to a single administration. * denotes a significant effect with $p < 0.05$.

Discussion

In this study we aimed for combining metabolomics in $brain_{ECF}$ and plasma with multivariate PK/PD modeling to obtain insight into the systems response, as well as to explore the target site of effect upon CNS drug administration. By integrating time-resolved metabolomics analysis with multivariate PK/PD, we revealed the diverse dynamical responses of biogenic amines and amino acids in $brain_{ECF}$ and plasma upon administration of the $D_{2/3}$ agonist QP. Indeed, the quantitative characterization of the system-wide biomarker responses showed a variety of *in vivo* potency and maximal response values in both $brain_{ECF}$ and plasma. Additionally, the unique evaluation of time-resolved metabolomics in both $brain_{ECF}$ and plasma revealed a few potential blood-based biomarkers reflecting effects in $brain_{ECF}$. Interestingly, it was also observed that many biochemical responses of QP have their main origin in the periphery rather than in the $brain_{ECF}$. Finally, our study showed no response of eight-day administration on biogenic amine and amino acid levels.

Exploration of target site and identification of blood-based biomarkers

It is a great challenge to identify blood-based biomarkers that reflect neurochemical responses in the brain. Often, these measurements are done at one time-point. In such case, however, correlations between plasma and $brain_{ECF}$ responses cannot reveal the causal relation. In the current study we were able to use the temporal delay between the $brain_{ECF}$ and plasma biomarker responses to identify the potential causal relation between them (i.e. the slowest response is likely a consequence of the quickest response via transport over the blood-brain barrier (BBB)). The BBB has multiple transport systems that transport biogenic amines and amino acids, for example, the large neutral amino acid transporter 1 (LAT1; for transport of e.g. glutamine, tyrosine, tryptophan), the cationic amino acid transporter 1 (CAT1; for transport of arginine and lysine), or the serotonin transporter (SERT; for transport of serotonin) (22,23). These transport systems exist at both the luminal and abluminal site of the BBB, whereby biogenic amines and amino acids can be transported from plasma to brain and vice versa. It is therefore likely that the parallel responses in plasma are, at least partially, explained by BBB transport. Interestingly, the number of biogenic amines transported from $brain_{ECF}$ to plasma was lower than those transported from plasma to brain (Table I). This observation it suggests first of all that, even if a drug does not cause a direct response in the brain (e.g. because of no exposure), biochemical responses may propagate from plasma to $brain_{ECF}$ and cause secondary responses. Second, the observed assymetry underlines the difficulty of finding blood-based markers reflective of drug responses in $brain_{ECF}$. 6 Potential blood-based biomarkers nevertheless reflected a response in $brain_{ECF}$ (Table I, Figure 1). Importantly, 5 of them showed non-linear transport over the BBB. It is advisable to take this non-linearity into account when evaluating blood-based biomarkers as a surrogate for an effect in $brain_{ECF}$. The blood-based biomarker response may be restricted by the maximal transport rate over the BBB and hence it

may affect the estimation of the maximal effect (E_{MAX}) parameter. Therefore, in order to understand the dynamics of the blood-based biomarker response in a clinical context, it is recommended to determine the relation between the plasma and $brain_{ECF}$ biomarker response preclinically similar to the current study.

The effects of eight-day QP administration

Interestingly, while there was a significant response upon eight-day administration of QP in PK/PD parameters describing the neuroendocrine response (18), no significant impact on basal biomarker levels was identified in the current study, although dopamine, DOPAC and HVA were only analyzed for experiment day 1. A possible explanation could be that the biological systems that underlie the amino acid and biogenic amine responses have greater flexibility than the neuroendocrine system in adapting to perturbations such as QP administration.

The effects of QP on multiple pathways

QP appeared to have an overall inhibiting response on multiple biogenic amine pathways. First of all, the dopamine metabolism in the $brain_{ECF}$ was inhibited, which could be explained by the response of QP on the D_2 autoreceptors located on the presynaptic neuron (24). Moreover, QP reduced peripheral phenylalanine concentrations, thereby lowering the brain levels of phenylalanine and tyrosine that constitute the basis of the dopamine metabolism. Second, although QP did not significantly affect cerebral glutamate levels, glutamate signaling may be inhibited by QP, given that glycine, serine, proline and putrescine levels in $brain_{ECF}$ were decreased, all acting as co-activator of the NMDA receptor (25,26).

Furthermore the reduction of the BCAA levels and the increase of DL-3-aminoisobutyric acid in plasma may both be associated with increased activity of the animals. BCAA levels were found negatively correlated with activity (27), while DL-3-aminoisobutyric acid was observed positively associated with activity (28). Indeed, QP does induce locomotion as measure of increased activity and movement (29), and the modified levels of BCAA and DL-3-aminoisobutyric acid in our study may be a reflection of that.

Finally, the reduction of histidine and histamine in plasma may reflect an inhibitory effect of QP on the immune system. Histamine is directly released from dendritic cells, macrophages and neutrophils upon production from histidine by the enzyme histidine decarboxylase (30). Interestingly, dopamine receptors are expressed in various immune cells such as dendritic cells, neutrophils and natural killer cells (31), indicating a potential mechanism through which QP may have influenced the histamine metabolism.

Some limitations of the current study

Of course we are aware of some limitations of this study. First of all, while the results in our study strongly indicate a systems wide response for the $D_{2/3}$ receptor agonist QP, it should be confirmed by using other D_2 agonists whether the observed responses are related to dopaminergic activity, and to which receptor subtype they are related. Such analysis would give insights into drug-class specific system-wide responses. For example, a multivariate analysis of several antipsychotic D_2 receptor agonists showed large neurochemical and behavioral overlap of clozapine with 5-HT_{2a} antagonists, but not haloperidol (32). Ultimately, the multivariate PK/PD approach may link *in vitro* and *in vivo* characterizations of drug-class related pharmacology by connecting the pattern of *in vivo* potencies to *in vitro* affinities.

Second, although the analytical platforms that have been used in the current study are well-developed with proven robustness (19,21), glycine measured by the targeted platform was described by cluster 3 dynamics, while the glycine response as analyzed by untargeted analysis was closer to the cluster 2 pattern (Figure 1). Inter-laboratory reproducibility is currently a topic of investigation, although early research suggests good robustness of metabolomics platforms towards this type of variation (33). An explanation could be non-linearity of the apparatus response given the fact that the untargeted analysis provided response ratios (analyte peak area/internal standard peak area), whereas the targeted analysis presented concentrations.

Third, although not only biogenic amines and amino acids are expected to respond to QP, we were limited by sample volume of the microdialysates. It would be valuable to extend the current approach with multiple platforms integrated to obtain a comprehensive insight into the system-wide effects of CNS drugs. Fortunately, the microdialysis-metabolomics technology is rapidly evolving, requiring lower sample volumes for metabolomics analysis (34,35). Furthermore, to counteract the high attrition rates in CNS drug development, it will be important to accurately monitor the pharmacology in early clinical drug development (3). Such monitoring needs accessible biomarkers that can be obtained from the blood, for example. The combined microdialysis-metabolomics technology is envisioned valuable and relatively low-cost to develop specific biomarker panels for CNS drugs (or drug classes).

Finally, all $brain_{ECF}$ measurements were made in the striatum. To gain insight into the higher hierarchy of the brain, the brain circuitry, it is essential to do measurements in multiple brain regions that are relevant to the drugs' mechanism of action. Indeed, CNS diseases and treatment responses are determined by the balance among signaling of multiple neurotransmitters in multiple regions (36–38). Addition of multiple brain regions

to a multivariate PK/PD model is therefore envisioned to further elucidate the systems pharmacodynamics of CNS drugs.

Conclusion

CNS drug development is challenged by low success rates and high development costs. Biomarker-driven drug development is seen as a logical step to improve these success rates, and metabolomics holds great promise in this regard. It provides a relatively low-cost method to comprehensively screen for drug response biomarkers. In this study we showed for the first time how time-resolved metabolomics analysis in combination with multivariate PK/PD describes the diverse dynamical patterns in $brain_{ECF}$ and plasma in a pharmacologically meaningful manner to evaluate systems-wide CNS drug effects. Moreover, our approach also enables to explore the target site of effect, as well as to identify blood-based biomarkers that are reflective of drug responses in $brain_{ECF}$. Further application and development of this method is envisioned to provide an important connection between drug discovery and early drug development.

References

1. Soares HD. The use of mechanistic biomarkers for evaluating investigational CNS compounds in early drug development. Curr Opin Investig Drugs. 2010;11(7):795–801.
2. Hurko O, Ryan JL. Translational research in central nervous system drug discovery. NeuroRx. 2005;2(October):671–82.
3. Morgan P, Van Der Graaf PH, Arrowsmith J, Feltner DE, Drummond KS, Wegner CD, et al. Can the flow of medicines be improved? Fundamental pharmacokinetic and pharmacological principles toward improving Phase II survival. Drug Discov Today. Elsevier Ltd; 2012;17(9/10):419–24.
4. Danhof M, Alvan G, Dahl SG, Kuhlmann J, Paintaud G. Mechanism-based pharmacokinetic-pharmacodynamic modeling-a new classification of biomarkers. Pharm Res. 2005;22(9):1432–7.
5. Lange ECM de, Brink WJ van den, Yamamoto Y, Witte WEA de, Wong YC. Novel CNS drug discovery and development approach: model-based integration to predict neuro-pharmacokinetics and pharmacodynamics. Expert Opin Drug Discov. Taylor & Francis; 2017;12(12):1207–18.
6. Greef J Van Der, Mcburney RN. Rescuing drug discovery: in vivo systems pathology and systems pharmacology. Nat Rev Drug Discov. 2005;4:961–8.
7. van der Greef J, Adourian A, Muntendam P, McBurney RN. Lost in translation? Role of metabolomics in solving translational problems in drug discovery and development. Drug Discov Today Technol. 2006;3(2):205–11.
8. Kaddurah-Daouk R, Kristal BS, Weinshilboum RM. Metabolomics: a global biochemical approach to drug response and disease. Annu Rev Pharmacol Toxicol. 2008;48:653–83.
9. Hayes RL, Robinson G, Muller U, Wang KKW. Translation of Neurological Biomarkers to Clinically Relevant Platforms. Methods Mol Biol. 2009;566:303–13.
10. Kaddurah-Daouk R, Weinshilboum R, Pharmacometabolomics Research Network. Metabolomic Signatures for Drug Response Phenotypes: Pharmacometabolomics Enables Precision Medicine. Clin Pharmacol Ther. 2015;98(1):71–5.
11. Burt T, Nandal S. Pharmacometabolomics in Early-Phase Clinical Development. Clin Transl Sci. 2016;9(3):128–38.
12. de Lange ECM. Recovery and Calibration Techniques: Toward Quantitative Microdialysis. Microdialysis in Drug Development. 2013. p. 13–33.
13. Ravenstijn PG, Drenth H-J, O'Neill MJ, Danhof M, de Lange EC. Evaluation of blood-brain barrier transport and CNS drug metabolism in diseased and control brain after intravenous L-DOPA in a unilateral rat model of Parkinson's disease. Fluids Barriers CNS. BioMed Central Ltd; 2012;9(4):1–14.
14. Qu Y, Olson L, Jiang X, Aluisio L, King C, Jones EB, et al. Evaluating PK/PD relationship of CNS drug by using liquid chromtography/tandem mass spectrometry coupled to in vivo microdialysis. Tandem Mass Spectrom Appl Princ. 2012;421–40.
15. Kohler I, Hankemeier T, Graaf PH Van Der, Knibbe CAJ, Hasselt JGC Van. Integrating clinical metabolomics-based biomarker discovery and clinical pharmacology to enable precision medicine. Eur J Pharm Sci. Elsevier; 2017;109S:S15–21.
16. van den Brink WJ, Hankemeier T, van der Graaf PH, de Lange ECM. Bundling arrows: improving translational CNS drug development by integrated PK/PD-metabolomics. Expert Opin Drug Discov. Taylor & Francis; 2018;0(0):1–12.
17. van den Brink WJ, Elassaiss-Schaap J, Gonzalez-Amoros B, Harms AC, van der Graaf PH, Hankemeier T, et al. Multivariate pharmacokinetic/pharmacodynamic (PKPD) analysis with metabolomics shows multiple effects of remoxipride in rats. Eur J Pharm Sci. 2017 Nov;109:431–40.
18. Brink WJ van den, Berg D-J van den, Bonsel FE, Hartman R, Wong Y-C, Graaf PH van der, et al. Fingerprints of CNS drug effects: a plasma neuroendocrine reflection of D2 receptor activation using multi-biomarker PK/PD modeling. Submitted. 2018;
19. Flik G, Folgering JHA, Cremers TIHF, Westerink BHC, Dremencov E. Interaction Between Brain Histamine and Serotonin, Norepinephrine, and Dopamine Systems: In Vivo Microdialysis and Electrophysiology Study. J Mol Neurosci. 2015;56:320–8.
20. Allers KA, Dremencov E, Ceci A, Flik G, Ferger B, Ittrich C, et al. Acute and Repeated Flibanserin Administration in Female Rats Modulates Monoamines Differentially Across Brain Areas : 2010;1757–67.
21. Noga MJ, Dane A, Shi S, Attali A, van Aken H, Suidgeest E, et al. Metabolomics of cerebrospinal fluid reveals changes in the central nervous system metabolism in a rat model of multiple sclerosis. Metabolomics. 2012;8(2):253–63.

22. Ohtsuki S, Terasaki T. Expert Review Contribution of Carrier-Mediated Transport Systems to the Blood–Brain Barrier as a Supporting and Protecting Interface for the Brain; Importance for CNS Drug Discovery and Development. Pharm Res. 2007;24(9):1745–58.
23. Marc DT, Ailts JW, Campeau DCA, Bull MJ, Olson KL. Neurotransmitters excreted in the urine as biomarkers of nervous system activity: Validity and clinical applicability. Neurosci Biobehav Rev. Elsevier Ltd; 2011;35(3):635–44.
24. Anzalone A, Lizardi-Ortiz JE, Ramos M, De Mei C, Hopf FW, Iaccarino C, et al. Dual control of dopamine synthesis and release by presynaptic and postsynaptic dopamine D2 receptors. J Neurosci. 2012;32(26):9023–34.
25. Ortiz JG, Cordero ML, Rosado A. Proline-glutamate interactions in the CNS. Prog Neuro-Psychopharmacology Biol Psychiatry. 1997;21(1):141–52.
26. Jänne J, Alhonen L, Keinänen T a, Pietilä M, Uimari A, Pirinen E, et al. Animal disease models generated by genetic engineering of polyamine metabolism. J Cell Mol Med. 2005;9(4):865–82.
27. Shimomura Y, Murakami T, Nakai N, Nagasaki M, Harris R a. Exercise promotes branched-chain amino acids catabolism: Effects of branched-chain amino acids supplementation on skeletal muscle during exercise. J Nutr. 2004;134(6):1583S–1587.
28. Roberts LD, Boström P, O'Sullivan JF, Schinzel RT, Lewis GD, Dejam A, et al. β-Aminoisobutyric Acid Induces Browning of White Fat and Hepatic β-oxidation and is Inversely Correlated with Cardiometabolic Risk Factors. Cell Metab. 2014;19(1):96–108.
29. Giuffrida A, Parsons LH, Kerr TM, Rodríguez de Fonseca F, Navarro M, Piomelli D. Dopamine activation of endogenous cannabinoid signaling in dorsal striatum. Nat Neurosci. 1999;2(4):358–63.
30. Thurmond RL. Histamine in Inflammation. 709th ed. Thurmond RL, editor. New York: Landes Bioscience and Springer Science+Business Media, LLC; 2010. 1-143 p.
31. Chandrani Sarkar, Basu B, Chakroborty D, Dasgupta PS, Basua S. The immunoregulatory role of dopamine: an update. Brain Behav Immunol. 2011;24(4):525–8.
32. Carlsson A, Waters N, Holm-waters S, Tedroff J, Nilsson M, Carlsson ML. Interactions between monoamines, glutamate, and GABA in schizophrenai: new evidence. Annu Rev Pharmacol Toxicol. 2001;41:237–60.
33. Siskos AP, Jain P, Römisch-Margl W, Bennett M, Achaintre D, Asad Y, et al. Interlaboratory Reproducibility of a Targeted Metabolomics Platform for Analysis of Human Serum and Plasma. Anal Chem. 2017;89(1):656–65.
34. Zestos AG, Kennedy RT. Microdialysis Coupled with LC-MS/MS for In Vivo Neurochemical Monitoring. AAPS J. The AAPS Journal; 2017;19(5):1284–93.
35. Zhou Y, Wong J-M, Mabrouk OS, Kennedy RT. Reducing Multifunctional Adsorption to Improve Recovery and In Vivo Detection of Neuropeptides by Microdialysis with LC-MS. Anal Chem. 2015;87(19):9802–9.
36. Qi Z, Yu GP, Tretter F, Pogarell O, Grace AA, Voit EO. A heuristic model for working memory deficit in schizophrenia . Biochim Biophys Acta. Elsevier B.V.; 2016;1860:2696–705.
37. Spiros A, Roberts P, Geerts H. A quantitative systems pharmacology computer model for schizophrenia efficacy and extrapyramidal side effects. Drug Dev Res. 2012;73(4):196–213.
38. Roberts P, Spiros A, Geerts H. A humanized clinically calibrated Quantitative Systems Pharmacology model for hypokinetic motor symptoms in Parkinson's disease. Front Pharmacol. 2016;7(FEB):1–14.

Supplement 1 – Equations

Inter-individual and residual variability

$$\vartheta_i = \vartheta_{pop} * e^{\eta i} \quad \text{(Eq. 1)}$$

$$Log(C_{obs\,,\,i\,,\,j}) = Log(C_{pred}\,,\,i\,,\,j) + \varepsilon_{i\,,\,j} \quad \text{(Eq. 2)}$$

$\boldsymbol{\vartheta_i}$ is the estimated parameter for individual i; $\boldsymbol{\vartheta_{pop}}$ is the estimated parameter for the population; $\boldsymbol{\eta_i}$ follows a normal distribution with mean 0 and variance ω^2; $\boldsymbol{C_{obs,i,j}}$ is the observed concentration data point for individual i at timepoint j; $\boldsymbol{C_{pred,i,j}}$ is the predicted concentration for data point for individual i at timepoint j; $\boldsymbol{\varepsilon_{i,j}}$ follows a normal distribution with mean 0 and variance σ^2.

Baseline models

No pattern

$$C_{MET\,,\,BSL} = BSL_{MET} \quad \text{(Eq. 3a)}$$

Linear decay function

$$C_{MET\,,\,BSL} = BSL_{MET} * (\,1 + s * time) \quad \text{(Eq. 3b)}$$

Exponential decay function

$$C_{MET\,,\,BSL} = (\,BSL_{MET} - BSL_{min}\,) * e^{-\,kdec\,*\,time} + BSL_{min} \quad \text{(Eq. 3c)}$$

$\boldsymbol{C_{MET,BSL}}$ is the biomarker concentration given no drug response; $\boldsymbol{BSL_{MET}}$ is the biomarker concentration at baseline at time = 0; $\boldsymbol{s}$ is the slope of the change in baseline with time; $\boldsymbol{BSL_{min}}$ is the minimum level of the basal biomarker levels; $\boldsymbol{k_{dec}}$ is the rate of baseline biomarker decay with time.

Drug response models

Linear model

$$E = slope * C_{QP} \quad \text{(Eq. 4a)}$$

E_{MAX} model

$$E = \frac{E_{MAX} * C_{QP}}{EC_{50} + C_{QP}} \quad \text{(Eq. 4b)}$$

$\boldsymbol{E}$ is the magnitude of drug response; ***Slope*** is the parameter that determines the strength of the drug response; $\boldsymbol{C_{QP}}$ is the drug concentration at the target site, either plasma or $brain_{ECF}$; $\boldsymbol{E_{MAX}}$ is the maximal response; $\boldsymbol{EC_{50}}$ is the drug concentration at half maximal response.

Link models

No transit compartment model

$$Tr = 1 \quad \text{(Eq. 5a)}$$

Transit compartment model

$$Tr = e^{ktr * time} * \frac{(k_{tr} * time)^{Ntr}}{e^{-Ntr} * \sqrt{2\pi} * N_{tr}^{Ntr+0.5})} \quad \text{(Eq. 5b)}$$

Turnover model (effect on biomarker release)

$$\frac{dC_{MET}}{dt} = k_{OUT} * C_{MET,BSL} * (1 + E * Tr) - k_{OUT} * C_{MET} \quad \text{(Eq. 6)}$$

Pool model (effect on biomarker release)

$$\frac{dC_{MET,pool}}{dt} = k_{OUT} * C_{MET,BSL} - k_{REL} * (1 + E * Tr) * C_{MET,pool} \quad \text{(Eq. 7a)}$$

$$\frac{dC_{MET}}{dt} = k_{REL} * (1 + E * Tr) * C_{MET,pool} - k_{OUT} * C_{MET,PL} \quad \text{(Eq. 7b)}$$

No response

$$C_{MET} = C_{MET,BSL} \quad \text{(Eq. 8)}$$

Tr describes the time delay of response using a transit compartment model (1 = no delay); $\boldsymbol{k_{tr}}$ is the rate at which the response goes through the transit compartments; $\boldsymbol{N_{tr}}$ is the number of transit compartments; $\boldsymbol{C_{MET}}$ is the biomarker concentration in plasma or brain$_{ECF}$; $\boldsymbol{k_{OUT}}$ is the hormone turnover rate; $\boldsymbol{C_{MET,POOL}}$ is the biomarker concentration in the pool; $\boldsymbol{k_{REL}}$ is the biomarker release rate from the pool into plasma or brain$_{ECF}$.

Brain transport models

$$k_{transp} = k_{transp} \quad \text{(Eq. 9a)}$$

$$k_{transp} = \frac{V_{max}}{k_m} + C_{MET,\,target} \quad \text{(Eq. 9b)}$$

$$k_{OUT,\,notTS} = k_{OUT,\,notTS} \quad \text{(Eq. 9c)}$$

$$k_{OUT,\,notTS} = \frac{V_{max}}{k_m} + C_{MET,\,notTS} \quad \text{(Eq. 9d)}$$

$$\frac{dC_{MET,\,notTS}}{dt} = k_{transp} * C_{MET,\,target} - k_{OUT,\,notTS} * C_{MET,\,notTS} \quad \text{(Eq. 9e)}$$

$\boldsymbol{k_{transp}}$ is the transport rate over the blood-brain-barrier from the target site to the other compartment; $\boldsymbol{V_{max}}$ the maximal rate with $\boldsymbol{k_m}$ being the concentration at 50% of the maximal rate; $\boldsymbol{k_{OUT,notTS}}$ is the elimination rate from the compartment that is not the target site compartment.

Significance score calculation

$$Significance\ score = OFV_{ref} - OFV_{test} - inv.\chi^2\left(1 - \frac{\alpha}{n_{biomarker}},\, df\right) \quad \text{(Eq. 10)}$$

$\boldsymbol{OFV_{ref}}$ is a model with no drug effect included and $\boldsymbol{OFV_{test}}$ is a model with the drug effect included. The $\boldsymbol{inv.\chi^2}$ calculates a penalty for additional parameters (***df***) in the drug effect model on basis of the significance threshold ($\boldsymbol{\alpha}$) divided by the total number of biomarkers ($\boldsymbol{n_{biomarker}}$), i.e. bonferroni-correction.

Supplement 2 – Elbow plots

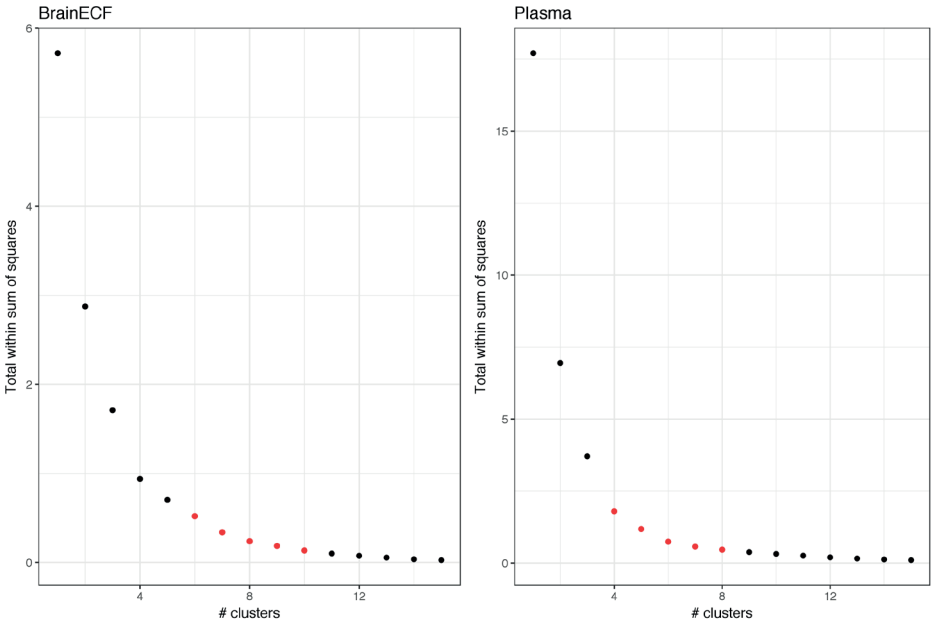

Figure S1. Elbow plots for the clustering of brain$_{ECF}$ (left) or plasma (right) responses. The elbow plot shows the balance between the number of clusters and the total variation that is explained by the clusters. The 'elbow' in this figure marks the point where adding another cluster does not further decrease the total unexplained variation, and is used to define the optimal number of clusters. While this is not always very clear from an elbow plot, a series of cluster numbers were selected, marked by the red dots, to subsequently be evaluated in a PK/PD cluster model.

Supplement 3 – Goodness-of-fit single biomarkers

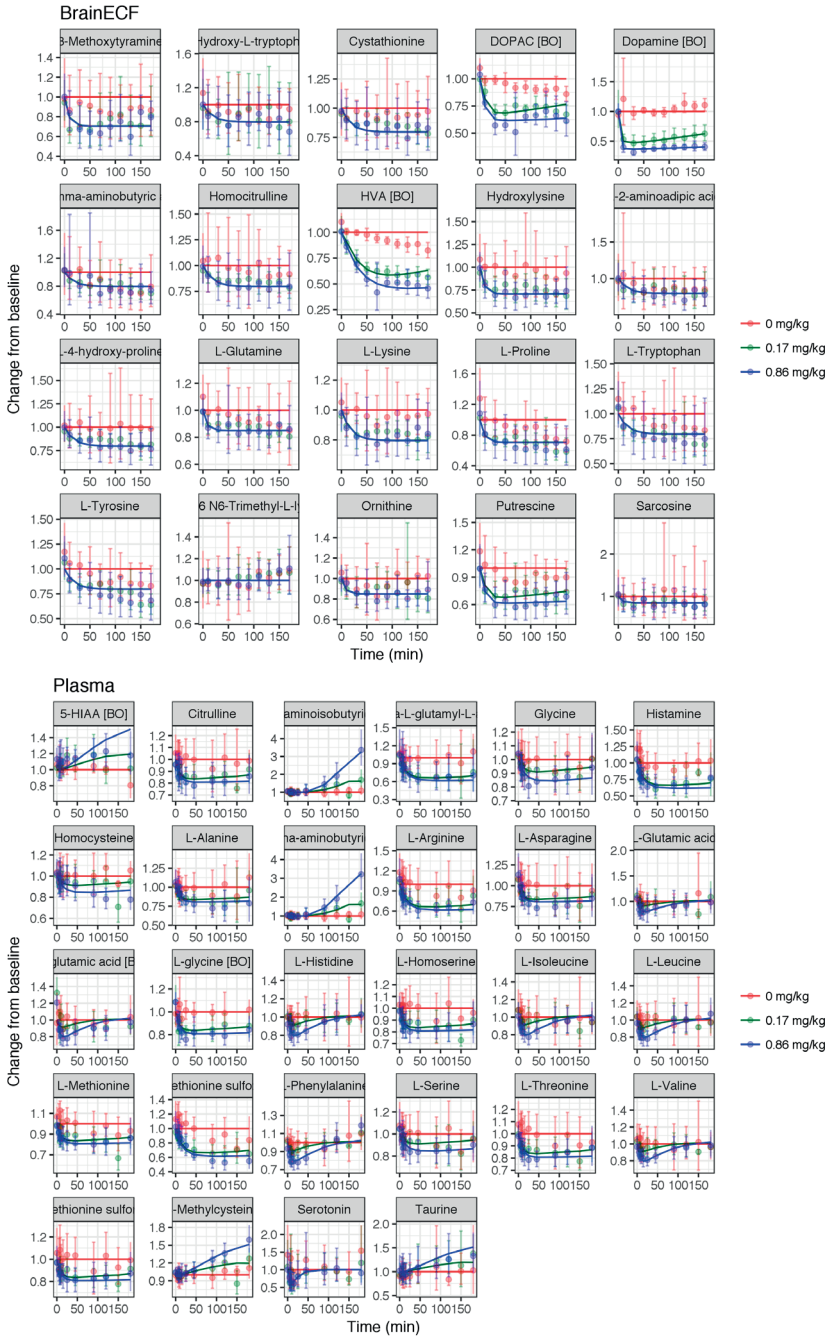

Figure S2. Goodness-of-fit of the cluster models on the baseline corrected single metabolite levels in brain$_{ECF}$ (top) and plasma (bottom). Dots are the geometric means per time point and dose, while the errorbars mark the geometric standard deviation. The lines represent the model-based predictions for 0 mg/kg (red), 0.17 mg/kg (green) and 0.86 mg/kg (blue).